JOURNAL OF MATERIALS SCIENCE 26 (1991) 1443–1453

The formation of β′-sialon from a montmorillonite–polyacrylonitrile composite by carbothermal reduction: an NMR, TGA, XRD and EM study

T. BASTOW, S. G. HARDIN, T. W. TURNEY
CSIRO Division of Materials Science and Technology, Locked Bag 33, Clayton 3168, Victoria, Australia

The products of carbothermal reduction in N_2 of a nanocomposite between dodecylammonium-exchanged montmorillonite and polyacrylonitrile (PAN) have been studied by solid-state ^{27}Al and ^{29}Si NMR spectroscopy, X-ray diffraction, transmission electron microscopy and thermogravimetry. Comparison with analogous reactions involving sodium-exchanged montmorillonite and dodecylammonium-exchanged montmorillonite (without PAN) shows that in the presence of PAN, the formation of silica, cordierite or mullite is almost completely suppressed. The only crystalline phase detected between 1000 and 1300 °C was a β′-sialon, having a much higher Si:Al ratio (7.05:1) than that of the precursor clay (2.44:1). Reduction of the octahedral AlO_6 begins near 1200 °C, forming increasing amounts of $Al(N,O)_4$ tetrahedra with temperature, so that by 1600 °C, complete reduction to AlN_4 (i.e. bulk AlN) has occurred. In contrast, reduction of the tetrahedral SiO_4 is appreciable at 1100 °C, and is almost complete (SiN_4 tetrahedra only) by 1200 °C. No intermediate $Si(N,O)_4$ environments are found. By 1600 °C, only the SiC_4 environment (i.e. bulk SiC) remains. A mechanism is suggested, involving the formation of alternating slabs of an amorphous aluminosilicate and carbon at 1000 °C, followed by diffusion of silicon from the outer regions of the aluminosilicate band towards the centre, and sequential reduction of $Si(OSi)_4$ and $Si(OSi)_3(OAl)$ groups.

1. Introduction

β′-sialons (silicon aluminium oxynitrides) have aroused considerable interest in recent years as refractory ceramic materials [1–3], particularly as alternatives to β-silicon nitride, from which they are derived by isomorphous replacement of (Si–N) by (Al–O) [4]; their properties and applications have been extensively reviewed [1, 3–5]. Production of β′-sialons from naturally occurring aluminosilicates by carbothermal reduction has been explored in several previous studies [6–12]. The mechanism of sialon formation from aluminosilicates by carbothermal reduction is still not fully understood [6, 9, 13–15]. Reactions involving montmorillonites having the general formula:

$$(Na, Ca)_{0.67}(Al, Fe, Mg)_4(Si, Al)_8O_{20}(OH)_4$$

have been shown to depend strongly on the temperature, the source of carbon and the atmosphere provided (argon or N_2) [16–18]. An approach developed by Kato and co-workers, using polyacrylonitrile (PAN) intercalation, has been shown to result in selective sialon formation at relatively low temperatures. Unlike analogous reactions involving physical mixtures of clay and carbon, the PAN–clay intercalate afforded very little mullite, alumina or silica [16, 17].

The value of solid-state magic-angle spinning (MAS) ^{27}Al and ^{29}Si nuclear magnetic resonance (NMR) has been demonstrated as a probe to investigate the structures and thermal reactions of aluminosilicates [19–23]. Chemical shift positions of ^{29}Si and ^{27}Al have been shown to be highly sensitive to the coordination number or environment of the nucleus (C, N or O) and the influences of the second coordination sphere [24–28]. A number of materials, including zeolites, montmorillonites and kaolinite have been studied [29–31]. These techniques have also been used to probe the structure of sialons in crystalline or glassy form [32, 33], and to monitor the formation of silicon carbide from a polysilane during pyrolysis [34].

This paper reports the conversion of a Wyoming montmorillonite to β′-sialon, via formation of a clay–organic molecular composite and its subsequent reduction.

2. Experimental procedure

2.1. Materials

Sodium nitrate (Univar), acrylonitrile (Unilab) and benzoyl peroxide (Technical) were from Ajax

0022–2461/91 $03.00 + .12

Chemicals. Dodecylamine (Puriss) was from Fluka Chemicals. A solution of dodecylammonium chloride was prepared from the amine by reaction with a stoichiometric amount of 12 M hydrochloric acid, followed by dilution to 0.1 M. AlN used as an NMR standard was from Cerac Inc. All other reagents and solvents were AR grade.

Sodium montmorillonite (Na-Mont) was prepared from Volclay Wyoming bentonite by the method of Attalla *et al.* [35]. The clay platelet size in the gel was mainly in the 1.2 to 1.5 μm range [36]. The gel (which yielded 1 g dry weight of clay per 13 to 18 g) was dried in air (16 h) at 100 °C, then ground and sieved to pass 80 mesh. Dodecylammonium montmorillonite (C_{12}-Mont) was prepared by dispersion of Na-Mont gel (10 g dry weight equivalent) in dodecylammonium chloride solution (0.1 M, 200 ml) and stirring (24 h) at room temperature. The material was separated by centrifugation and washed repeatedly with hot (approx. 80 °C) water on a filter until free of excess electrolyte. The exchange and washing procedure was repeated, after which the product was dried in air at 100 °C, ground and sieved to pass 80 mesh.

Dodecylammonium montmorillonite–polyacrylonitrile composite (C_{12}-Mont/PAN) was prepared by dispersion of C_{12}-Mont (25.0 g) in a mixture of toluene (400 ml) and acrylonitrile (100 ml), containing benzoyl peroxide (0.50 g) as initiator. The mixture was stirred under reflux for 2 days, filtered, and the product washed with toluene (2 × 100 ml), then light petroleum (2 × 100 ml), and finally air-dried at room temperature. The yield of pale yellow powder was 62.3 g. The powder was pressed to cylindrical tablets (3 g each, 19 mm diameter, 10 mm length).

2.2. Reduction procedure

Samples (approx. 3 g each) were heated in Al_2O_3 boats in a tube furnace fitted with a nitrogen flow system, with an approximate flow rate of 500 ml min^{-1} (approx. linear velocity 10 cm min^{-1}). Samples heated at temperatures up to 1000 °C were ramped quickly (500 °C h^{-1}) and held at the final temperature for 6 h, before cooling to ambient in N_2. Samples heated to higher temperatures were pre-heated at 1000 °C (6 h) as above, before ramping at 200 °C h^{-1} to the final temperature, holding for 12 h, and finally cooling in N_2.

2.3. Sample characterization

NMR measurements were made using a Bruker MSL 400 spectrometer in a nominal field of 9.4 T at frequencies of 104.268 MHz for ^{27}Al and 79.489 MHz for ^{29}Si. MAS spectra were obtained from Fourier transforms of the free induction decay following a $\pi/2$ pulse. The MAS rotation frequency was typically 4 kHz and the $\pi/2$ pulse length was 2 μsec for ^{27}Al and 4 μsec for ^{29}Si. Pulse repetition times were 5 sec for both nuclei. Generally 1000 to 2000 scans were accumulated for each ^{27}Al or ^{29}Si spectrum, using a custom-built aluminium-free Bruker MAS probe. The sample spinner capsule was made from magnesia-stabilized zirconia. The chemical shift reference compounds were Zeolite A for ^{27}Al (set at 58.6 p.p.m. relative to $Al(H_2O)_6^{3+}$) and TMS (0 p.p.m.) for ^{29}Si.

The relatively high iron content (2.7 wt %) of Wyoming montmorillonite resulted in separation of ferromagnetic impurities during carbothermal reduction of C_{12}-Mont/PAN samples, making subsequent observation of NMR spectra impossible. Hence, after reduction, these samples were calcined in air at 650 °C for 2 h to remove unreacted carbon [17], then extracted with refluxing 3 M HCl for 0.5 h [7, 12]. The latter procedure removed all ferromagnetic impurities, and enabled spectra to be obtained. Samples derived from Na-Mont and C_{12}-Mont were treated similarly for the sake of uniformity.

Powder X-ray diffraction (XRD) data were obtained with a Siemens D-500 diffractometer (Cu$K\alpha$ radiation, scan step 0.04°). Patterns were measured as bulk powders (all samples) and/or dried, layered suspensions on glass slides (unfired and 600 °C fired samples). XRD data were taken after decarbonization and acid extraction procedures, unless otherwise indicated.

Transmission electron microscopy (TEM) was carried out with a Jeol JEM-100CX electron microscope. Samples were dispersed in alcohol and examined against a holey carbon background. With the exception of the unfired C_{12}-Mont/PAN sample, all TEM data were collected after decarbonization and acid extraction procedures (so as to allow direct comparison with NMR data).

Thermal analyses were carried out with a Stanton-Redcroft STA-780 simultaneous TG–DTA instrument. Samples were heated from ambient temperature to 1000 °C at 10 °C min^{-1} in N_2.

Elemental analyses were performed by atomic absorption spectroscopy (AAS), on samples digested in $HF–H_2SO_4$, evaporated to dryness and then dissolved in HCl prior to determination. Silicon was determined gravimetrically by fusion with an $Na_2CO_3–K_2CO_3–H_3BO_3$ mixture, followed by extraction with aqueous HCl and weighing as SiO_2. The presence of iron (in HCl leaching solutions) was detected by testing with dilute KSCN solution; a deep red colour indicated a positive result.

3. Results and discussion

3.1. Sample preparation

Samples of Na-Mont and C_{12}-Mont were prepared as dense, finely divided powders. Although the sodium form was dispersible in aqueous media, the C_{12} form was hydrophobic and dispersed only in polar organic solvents, such as acetone. After heating in nitrogen to 600 °C or higher, both materials formed grey powders; the C_{12} form was virtually free of carbon (showing little or no weight change after decarbonization). Heating at 1300 °C or above resulted in a fused, glassy mass. In no case did heating result in ferromagnetic samples, indicating that metallic iron was not formed during the process. Subsequent air calcination yielded pale brown powders, from which very little iron was removed by acid extraction.

Samples of C_{12}-Mont/PAN were prepared as voluminous, pale yellow powders; the organic content (determined by weight loss on calcination to 650 °C) was 65 wt %. The material dispersed only in polar organic solvents (e.g. acetone). The extremely low free-flow density of the powder necessitated pressing into tablets prior to reaction. Heating in nitrogen resulted in the evolution of copious amounts of tar, leaving a black residue, which contained approximately 50 wt % carbon. Samples heated to 1000 °C or above became ferromagnetic. Subsequent air calcination of samples at 650 °C yielded pale brown to grey powders. Extraction with 3 M HCl then gave grey powders which were paramagnetic, with the yellow extracts giving a strong positive SCN^- test for Fe^{3+}.

3.2. Elemental analyses

Elemental analyses for Na-Mont, C_{12}-Mont and C_{12}-Mont/PAN samples are shown in Table I. Comparison of results for unfired samples of Na-Mont and C_{12}-Mont indicated that most (but not all) of the Na^+ and Ca^{2+} ions had been removed by ion-exchange of the sodium form with dodecylammonium chloride solution. The relative atomic ratios of the other elements (present as aluminosilicate framework ions) remained almost unchanged. Heat treatment of C_{12}-Mont at 600 °C or higher resulted in almost complete loss of carbon as organics, with the relative atomic ratios of the framework elements remaining essentially unchanged. Attempted iron extractions for Na-Mont and C_{12}-Mont were unsuccessful, presumably since the iron remained as tightly-bound silicates in these samples.

Analyses for C_{12}-Mont/PAN samples indicated that sodium and magnesium were lost progressively with increasing temperature. Magnesium has been reported to be removed as the volatile metal by carbothermal reduction, especially at temperatures in excess of 1300 °C [17]. A similar fate probably occurred for sodium. Levels of calcium remained low throughout, becoming almost negligible for the sample heated to 1600 °C. This was most likely due to formation of CaC_2 at elevated temperatures, followed by its conversion to CaO during decarbonization, and subsequent removal during acid extraction.

Iron removal by HCl extraction was more successful for the 1000 °C sample than for the 600 °C sample, reflecting an increasing amount of metallic material produced by carbothermal reduction. For the samples heated to 1300 and 1600 °C, a slight increase in residual iron levels was observed (after extraction), when compared with the 1000 °C sample. This may have been due to part of the metallic iron reacting further to produce small amounts of ferrosilicon and/or iron carbides, which were less susceptible to acid attack than the metal. These materials are thought to form as by-products during the carbothermal reduction of iron-rich clays [37]. However, such phases were not observed by XRD in the current work.

Comparison of the Si:Al atomic ratio for the C_{12}-Mont/PAN sample heated to 1300 °C with those for unfired Na-Mont and C_{12}-Mont indicates that considerable loss of aluminium had occurred in the former sample. This is believed to be a result of dissolution of finely-divided or poorly crystalline aluminium-containing material during the acid extraction step.

There is a report that the Si:Al ratio for montmorillonite–PAN complexes heated for 2 h under N_2 at temperatures between 1300 and 1500 °C remained constant at a value similar to that of the starting clay [17]. However, no acid extraction was used after carbothermal reduction. Other workers have reported that the degree of aluminium loss in sialons following extraction with boiling 3 M HCl is small, provided that the extraction time does not exceed half an hour [8].

Thus, it is suggested that loss of aluminium observed in the 1300 °C sample occurs mainly by acid dissolution of an amorphous and impure aluminium oxide (remaining from incomplete reduction) and/or X-ray amorphous AlN or aluminium oxynitrides co-produced in the reduction. The overall Si:Al ratio (after extraction) was 7.05. If pure β′-sialon, $Si_{6-z}Al_zO_zN_{8-z}$, were formed, this would result in a z value of 0.745 (calcd. 7.15% Al; 52.5% Si). The presence of aluminium-containing impurities in the sample (even after acid extraction) is probable, however, implying an even lower z value for this sialon. In contrast, an Si:Al ratio of 2.44 (as found in unfired Na-Mont) would be expected to give rise to a sialon of z value 1.744 (calcd. 16.68% Al; 42.37% Si).

The sample heated to 1600 °C was almost free of sodium, magnesium and calcium. The very low aluminium content of this sample is ascribed to extensive acid dissolution of aluminium-containing phases.

3.3. Thermal analyses

Thermal analysis of Na-Mont (Fig. 1a) showed an endothermic weight loss of 2.8% up to 150 °C attributed to loss of interlayer water. A second endotherm (3.7% loss) in the range 575 to 725 °C corresponded to dehydroxylation, as found in other studies [31, 38]. An exotherm centred at 943 °C was associated with collapse of the layer structure and the formation of an X-ray amorphous phase (see XRD results), without change in mass [39].

C_{12}-Mont (Fig. 1b) showed a more complex thermal curve; an endotherm centred at 382 °C (13.7% loss) corresponded to decomposition of the dodecylammonium ion. Decomposition of alkylammonium ions in clays has been noted to begin below 250 °C [40]. A second, sharp endotherm centred at 488 °C (no mass loss) may be associated with collapse of the basal spacing, after removal of the alkylammonium ions (see below). The third, broad endotherm (centred at 625 °C, 3.7% mass loss) was probably due to dehydroxylation, whilst an exotherm near 912 °C (no mass loss) was again assigned to structure collapse to an amorphous phase.

The thermal curve of C_{12}-Mont/PAN (Fig. 1c) was dominated by a broad area of mass loss (35.8%)

TABLE I Elemental analyses

Sample	Reaction temperature[a] (°C)	Composition (wt %)						Atomic ratio, Si:Al
		Na	Mg	Ca	Al	Si	Fe	
Na-Mont	25[b]	1.63	1.50	0.48	11.5	29.2	2.72	2.44
Na-Mont	600	–	–	–	–	–	2.7	–
C_{12}-Mont	25[b]	0.02	1.27	0.008	10.6	25.0	2.4	2.27
C_{12}-Mont	1000	0.04	1.45	0.014	12.7	–	2.8	–
C_{12}-Mont/PAN	600	0.05	0.71	0.014	10.7	–	2.0	–
C_{12}-Mont/PAN	1000	0.35	0.28	0.019	6.0	–	0.22	–
C_{12}-Mont/PAN	1300	0.26	0.38	0.11	6.70	49.2	0.52	7.05
C_{12}-Mont/PAN	1600	0.009	0.025	0.005	3.7	–	0.52	–

[a] All samples decarbonized in air and extracted with HCl prior to analysis unless indicated otherwise.
[b] No heat treatment, decarbonization or HCl extraction.

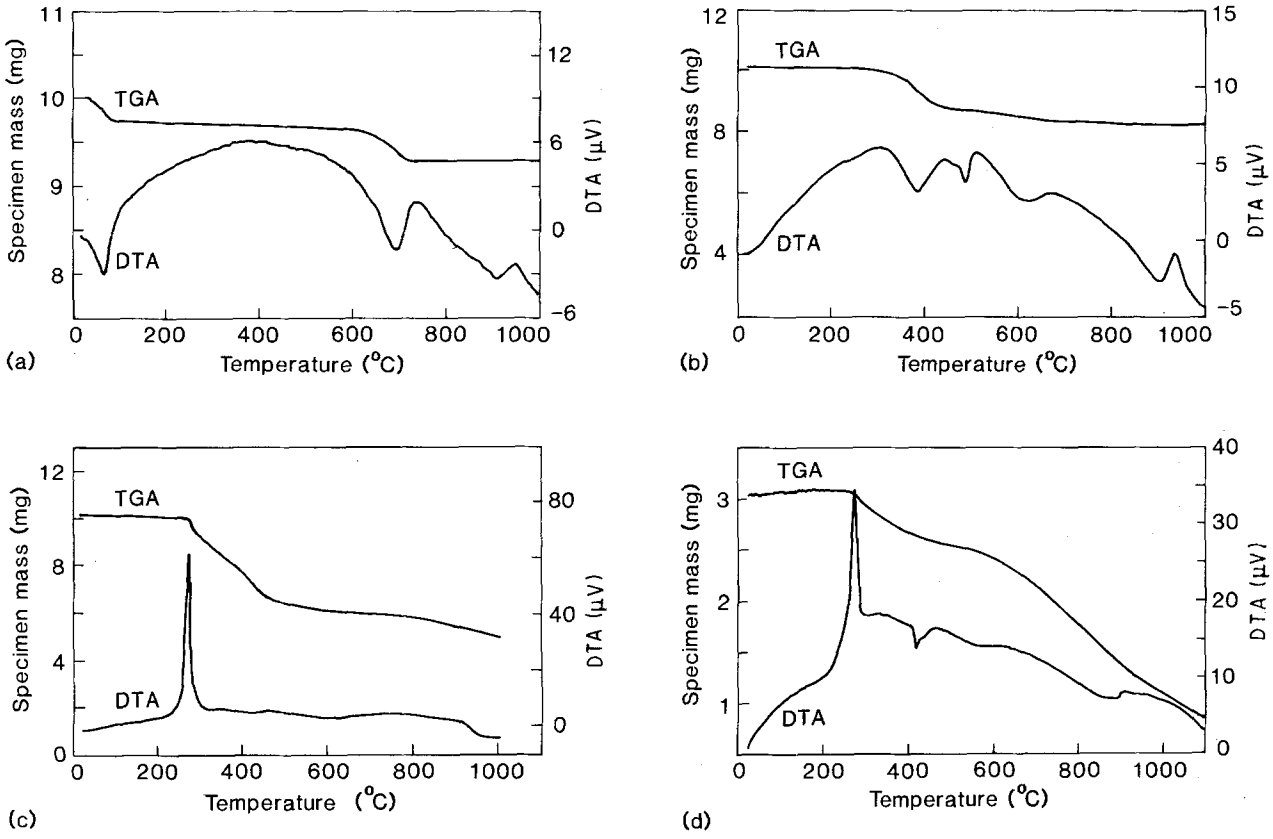

Figure 1 Thermogravimetric (TGA) and differential thermal (DTA) analyses of (a) Na-Mont, (b) C_{12}-Mont, (c) C_{12}-Mont/PAN and (d) PAN.

between 228 and 495 °C, which consisted of two overlapping components of roughly equal size centred near 270 and 400 °C, respectively. The former was exothermic, and may have corresponded to cyclization of a linear PAN to a graphite precursor [41], together with decomposition of the dodecylammonium ion. The second component resulted in very little energy change, and probably corresponded to further decomposition of the PAN, together with desorption of organics derived from the dodecylammonium ion. Unlike C_{12}-Mont, there was no sharp endotherm near 488 °C, suggesting that residual interlayer carbon prevented sudden collapse of the clay layers at this temperature. No distinctive endotherms due to dehydroxylation alone (expected near 600 °C), or exotherms due to complete structure collapse (expected near 900 °C) could be seen in the curve, unlike that for Na-Mont. However, such fine structure in the thermal curve may be obscured by the high organic content of the sample. Thus, a continuous mass loss of 14.6% between 495 and 1000 °C was attributed to further decomposition of organics and the resultant desorption of volatiles, together with dehydroxylation, leaving an aluminosilicate–carbon composite.

Thermal analysis of PAN itself (Fig. 1d) gave rise to a curve displaying a sharp exotherm at 272 °C, similar to that of the C_{12}-Mont PAN sample, followed by a small, sharp endotherm at 418 °C of uncertain origin. No other distinct endotherms or exotherms occurred above this temperature. There were two broad regions of mass loss, lying between 200 and 600 °C (17% mass loss) and 600 to 1000 °C (60% mass loss). Once again, these probably corresponded to cyclization, followed by evolution of organics, leaving a carbon residue.

TABLE II Phases observed by XRD from Na-Mont, C_{12}-Mont and C_{12}-Mont/PAN by heat treatment in N_2 at various temperatures

Reaction temperature (°C)	Na-Mont	C_{12}-Mont	C_{12}-Mont/PAN
25[a]	Na-Mont d_{001} = 1.27 nm	C_{12}-Mont d_{001} = 1.70 nm	d_{001} > 3.0 nm
600	d_{001} = 0.97 nm	d_{001} = 0.98 nm d_{001} = 0.95 nm[b]	d_{001} = 0.99 nm d_{001} = 2.41 nm[b]
1000	α-Cristobalite Trace mullite	Quartz α-Cristobalite Trace mullite	Traces α-cristobalite and mullite Trace graphite[b]
1100	–	–	β′-Sialon Trace quartz
1200	–	–	β′-Sialon Trace α-cristobalite
1300	Mullite Cordierite Trace α-cristobalite	Mullite Cordierite α-Cristobalite	β′-Sialon β′-Sialon[b] Graphite
1600			SiC cubic (3C) AlN hexagonal
	–	–	SiC cubic (3C)[b] AlN hexagonal Graphite

[a] No heat treatment, decarbonization or HCl extraction.
[b] Samples before decarbonization/iron extraction.

3.4. X-ray diffraction

The thermal reactions of montmorillonites have been well studied by XRD [17, 38, 42–45], and correlate closely with the main features observed here for Na-Mont (Table II). Hence, by 600 °C, dehydroxylation of the Na-Mont caused a decrease in interlayer spacing, d_{001}, from 1.27 to 0.97 nm. By 1000 °C, all clay structure had disappeared, and separation of α-cristobalite (JCPDS No. 11-695) and poorly-crystalline mullite (JCPDS No. 15-776) had occurred. By 1300 °C, the sample had fused to a glassy mass; both mullite and cordierite (JCPDS No. 12-294) could be detected. The latter is a common thermal decomposition product of magnesium-rich clays [39]. The amount of α-cristobalite had decreased (compared with the sample heated to 1000 °C), presumably due to its reaction with Na^+ to form silicate glasses in the melt.

The behaviour of C_{12}-Mont paralleled that of Na-Mont up to 600 °C. Thus, at this latter temperature, evolution of organics and dehydroxylation was nearly complete, and an interlayer spacing of only 0.95 nm was found, before decarbonization, and a value of 0.98 nm after treatment, similar to that of Na-Mont at the same temperature. This implied the absence of interlayer carbon after heating to 600 °C, even before decarbonization treatment. At 1000 °C, both quartz (JCPDS No. 33-1161) and α-cristobalite were present. The thermal stability of quartz was increased by the low concentrations of Na^+ in C_{12}-Mont; no quartz was observed for Na-Mont at this temperature. The relative thermal stabilities of quartz and α-cristobalite are known to be dependent on cationic impurities [2]. By 1300 °C, however, no quartz was found, but only α-cristobalite, mullite and cordierite. The relative amount of α-cristobalite observed at 1300 °C was greater for C_{12}-Mont than for Na-Mont; presumably larger amounts of low-melting sodium and calcium silicate glasses were formed in the latter.

The phases formed from C_{12}-Mont/PAN were markedly different to those formed from its two precursors. At room temperature, a poorly-defined XRD, with a rising baseline in the 3 nm region, was obtained. At 600 °C (before decarbonization and iron extraction), an interlayer spacing d_{001}, of 2.41 nm was observed, indicating the presence of large amounts of interlayer carbon. After decarbonization, however, a basal spacing of 0.99 nm was found, comparable to the spacings for Na-Mont and C_{12}-Mont at this temperature. By 1000 °C (before decarbonization), a mainly amorphous material resulted, containing only traces of quartz, α-cristobalite, and a broad absorption at 0.34 nm due to poorly crystalline graphite. The latter peak disappeared on decarbonization. The clay structure had collapsed by 1000 °C, as expected [39].

Reduction of the silicate framework began above 1000 °C, with increasing amounts of β-Si_3N_4 (JCPDS No. 33-1160) and/or β′-sialon phases (JCPDS No. 36-1333) being formed between 1100 and 1300 °C. Previous workers have also noted the formation of β′-sialon phases at temperatures as low as 1100 °C, when using an intercalation approach [16]. In the present study, only trace amounts of quartz and α-cristobalite were seen at 1100 and 1200 °C, respectively; these had disappeared by 1300 °C. No mullite, cordierite or sialon phases other than β′ were observed.

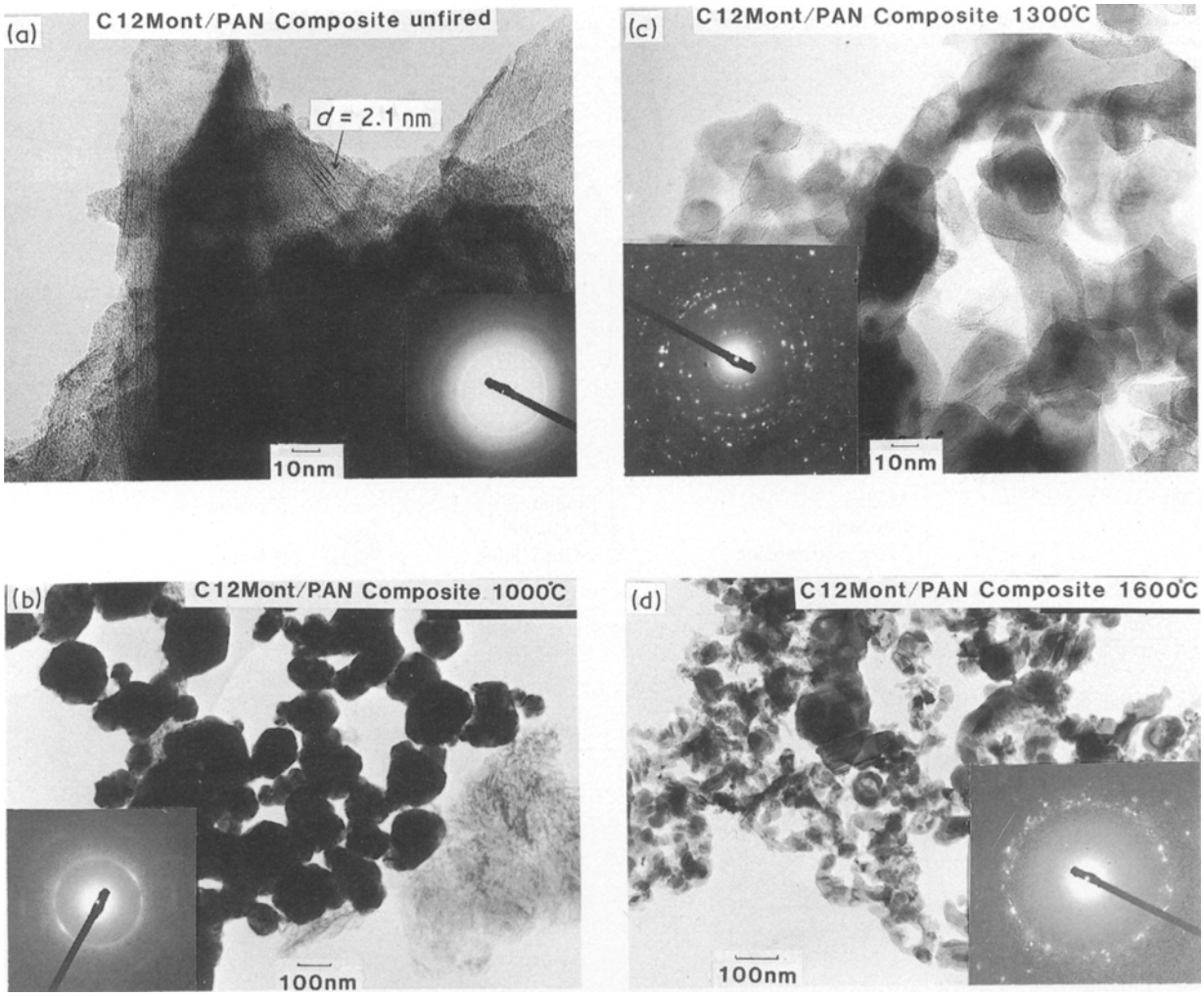

Figure 2 Transmission electron micrographs and selected-area diffraction patterns of C_{12}-Mont/PAN (a) unfired, and after heating to (b) 1000 (c) 1300 and (d) 1600 °C.

Calculations based on a hexagonal unit cell gave the following dimensions for β′-sialon (1300 °C sample):

$$a = 0.7619 \text{ nm}, \quad c = 0.2917 \text{ nm}$$

[β-Si_3N_4: $a = 0.76044$ nm, $c = 0.29075$ nm]

[β′-$Si_3Al_3O_3N_5$: $a = 0.76781$ nm, $c = 0.29769$ nm]

Assuming a linear relationship (Vegard's Law) between cell dimensions and aluminium concentration for the β′-sialon solid solution series, a z value of 0.58 (using a values) or 0.41 (using c values) was obtained, and was lower than that calculated from elemental analyses (0.745). The lower z value obtained from XRD analysis is consistent with the presence of some of the aluminium as amorphous or very poorly crystalline non-sialon phases.

By 1600 °C, complete conversion to hexagonal AlN (JCPDS No. 25-1133) and cubic SiC (3C polytype, JCPDS No. 29-1129) had occurred. As with the 1000 °C sample, XRD patterns of higher-temperature samples before decarbonization showed peaks at 0.345 and 0.199 nm characteristic of graphite, which disappeared after decarbonization at 650 °C, with no other change to the pattern.

No XRD evidence was found for the separation of crystalline alumina at any temperature, or of AlN at 1300 °C or below. However, the presence of an amorphous impure alumina resulting from incomplete reduction of the octahedral aluminium layer in the clay, or from the intermediate $MgAl_2O_4$ (see below) is likely. The formation of poorly crystalline AlN and/or aluminium oxynitrides at 1300 °C or lower also cannot be ruled out. The latter are expected to be highly susceptible to acid extraction procedures. No crystalline magnesium-containing phases were observed at any stage.

3.5. Electron microscopy

Transmission electron micrographs and selected-area diffraction (SAD) patterns of C_{12}-Mont/PAN samples heated to various temperatures are shown in Fig. 2. The fragmentation of samples into separate phases is most likely caused by evolution of CO_2 occurring during decarbonization treatment.

Unfired samples (Fig. 2a) showed a morphology consisting of thin flakes, approximately 0.5 to 1 μm in size, similar to that of untreated Na-Mont. SAD indicated randomly oriented material with spacings at 0.24 nm ($d_{2\,0\,0}$, $d_{1\,3\,0}$) and 0.42 nm ($d_{0\,2\,0}$). No external (non-intercalated) PAN was seen in this sample; free

PAN when prepared in the absence of clay displays a morphology consisting of fine (< 0.1 μm) fluffy particles.

The morphology of C_{12}-Mont/PAN after heating to 600 °C remained similar to that of the unfired sample, indicating the persistence of clay-like structure at this temperature. The SAD once again indicated randomly oriented particles (uniform diffuse rings) with similar spacings to those of the unfired sample.

At 1000 °C a minor phase, consisting of small, dense, roughly cubic particles (0.2 μm approx. size) had separated (Fig. 2b). The SAD of this phase showed spacings close to those of $MgAl_2O_4$ (JCPDS No. 21-1152), even though no such phase was observed by XRD; this was possibly due to poor crystallinity. The major phase was flakes around 1 μm in size, with an SAD indicating randomly oriented particles with a collapsed clay structure ($d_{0\,2\,0}$ = 0.413 nm).

With increasing temperature, the amount of the flake-like phase decreased (although the size of the individual flakes increased to nearly 2 μm) until 1300 °C, when complete disappearance of the clay-like phase had occurred. At 1100 °C and higher, a crystalline, irregularly-shaped plate-like phase (0.05 to 0.10 μm size range) appeared and increased in abundance, becoming dominant by 1300 °C. Diffraction indicated that this was isomorphous with β-Si_3N_4. Direct measurement of lattice projections in the [h 0 l] direction from high-magnification micrographs gave spacings of about 0.6 nm (cf. $d_{0\,1\,0}$ = 0.665 nm for β′-sialon, z = 3); these values were within the uncertainty (20%) in the true magnification value of the micrographs. In the 1100 to 1300 °C range, a very small amount of fibrous impurity (< 1% of total material) was also observed (width 0.03 to 0.1 μm, length 2 to 8 μm), which was attributed to the crystallization of needle-like mullite [2]. Due to progressive loss of magnesium as the metal on carbothermal reduction [17], the cubic spinel phase seen at 1000 °C was absent after heating to higher temperatures. In its place, a small amount of amorphous plate-like phase (no SAD pattern observable) was seen (0.05 to 0.1 μm size range). This material may be impure amorphous alumina derived from reduction of $MgAl_2O_4$, as well as unreacted material derived from the octahedral Al–O layer originally present in the clay. Very poorly crystalline AlN and its acid hydrolysis products (the latter resulting from the HCl extraction procedure) may also be present. Residual sodium, magnesium, calcium and iron probably contribute to this amorphous phase; traces of sodium and calcium may retard the reduction of the alumina contained therein until a relatively high temperature (near 1600 °C).

By 1600 °C, the product consisted almost entirely of irregular plate-like particles (0.05 to 0.1 μm size range). No lattice images could be discerned from high-magnification micrographs. The SAD of this phase was that expected for a mixture of poorly crystalline SiC and AlN. A few particles of a "rope-like" phase, (< 1% of total) were seen (0.2 μm width, 4 μm length approx.), probably derived from reduction of mullite fibres; none of the latter remained. A trace of a phase appearing as small whiskers (0.03 μm × 3 μm) was observed, although such material was in insufficient quantity for characterization.

3.6. Nuclear magnetic resonance

The nomenclature used to describe ^{29}Si coordination environments in silicate sites is that devised by Engelhardt *et al.* [46, 47]. Using this convention, a silicon atom attached to four oxygens is designated Q. A superscript indicates the number of bridges (via oxygen) to other silicons. Substitution of an OSi group by an oxygen bridge to a different tetrahedral element (usually aluminium) is denoted in brackets. Oxygen bridges to protons or octahedral nuclei are not denoted. Thus, for example, the silicon nucleus in montmorillonite is denoted Q^3(0Al), indicating attachment to three other OSi groups. The fourth bridge is to octahedral aluminium, magnesium or iron (not tetrahedral aluminium).

Due primarily to field gradient effects of Fe^{3+}, Mg^{2+} and H^+ on the silicon and aluminium nuclei, an amount generally less than 20% of the total ^{27}Al content, and less than 5% of the total ^{29}Si content of clays, is observed [29]. Furthermore, species such as five-coordinated aluminium may be unobservable due to rapid relaxation times. Thus, when analysing ^{27}Al and ^{29}Si NMR spectra, it should be noted that relative peak areas or heights are of qualitative value only, and cannot be reliably used to measure molar ratios of species [29].

The ^{29}Si NMR spectrum of Na-Mont at room temperature (Fig. 3) showed a sharp, strong absorption at − 93 p.p.m. assigned to a silicon of the Q^3(0Al) type, while a slight inflection at − 106 p.p.m. due to a trace of highly silicious impurity, Q^4(0Al), was also apparent [22, 27, 29]. After dehydroxylation at 600 °C, an absorption appearing at − 100 p.p.m. could be assigned to Q^4(1Al), implying the formation of $(OSi)_3Si$–O–Al (tetrahedral) links after loss of –OH groups in the octahedral layer. The minor impurity of SiO_2 at − 107.7 p.p.m. persisted. This behaviour differed from a magnesium-rich montmorillonite in which the ^{29}Si resonance position was unchanged after dehydroxylation [29]. Separation of poorly crystalline mullite (− 86.6 p.p.m., Q^4(4Al)) [48] and α-cristobalite (− 110.9 p.p.m., Q^4(0Al)) [49] occurred at 1000 °C. By 1300 °C, fusion of the sample resulted in a broad absorption at − 106 p.p.m. (Q^4(0Al)), mainly due to glassy silica [48] with a shoulder at − 88 p.p.m. (Q^4(4Al)) due to mullite.

The ^{27}Al NMR spectra of Na-Mont (Fig. 4) showed a strong resonance near 0 p.p.m. due to an octahedral AlO_6 environment and a weak shoulder near 60 p.p.m., attributed to traces of tetrahedral aluminium isomorphously substituted into the SiO_4 framework [29]; these resonances persisted after heating the sample to 600 °C. The spectrum of the material after heating to 1000 °C showed a large increase in the AlO_4 resonance together with a slight decrease in AlO_6 intensity; this is most likely due to separation of aluminium into poorly crystalline mullite; this phase is known to contain both AlO_4 and AlO_6 environments

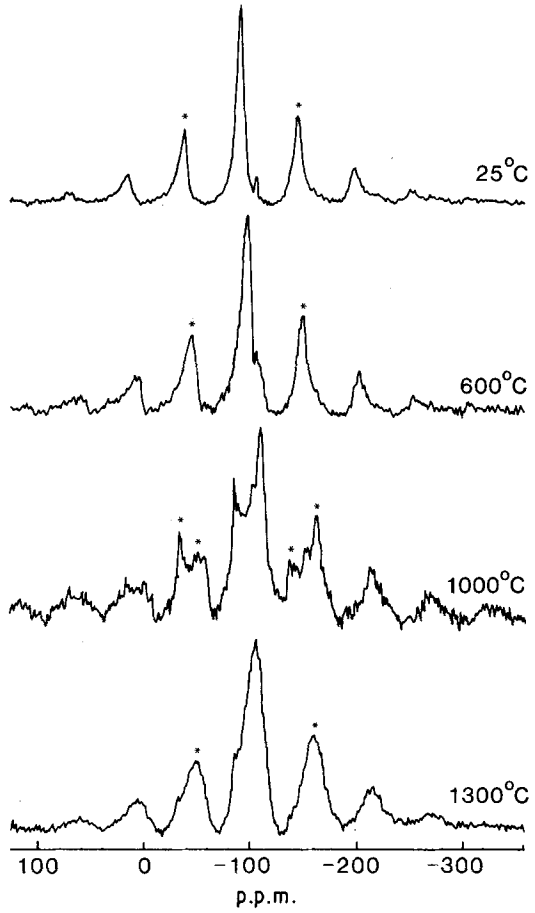

Figure 3 ^{29}Si NMR spectra of Na-Mont after heating to various temperatures; (*) spinning sidebands.

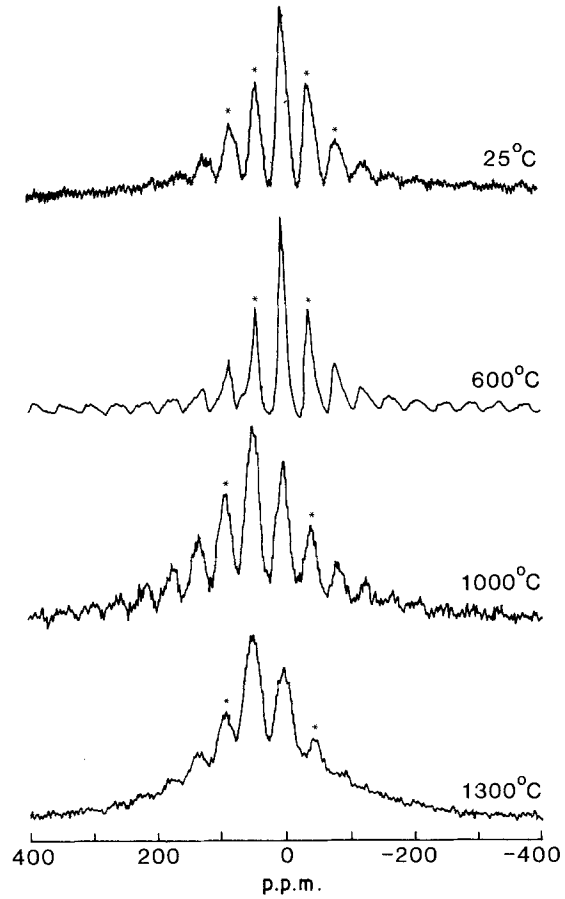

Figure 4 ^{27}Al NMR spectra of Na-Mont after heating to various temperatures; (*) spinning sidebands.

[39]. After sample treatment at 1300 °C, the NMR resonances remained similar, consistent with a mixture of mullite and cordierite [39] (both also observed by XRD).

After heating, samples derived from C_{12}-Mont/PAN displayed ^{29}Si NMR spectra (Fig. 5) very different to those of Na-Mont. After dehydroxylation at 600 °C, a splitting into Q^4(1Al) at −98.1 p.p.m. and Q^4(0Al) at −107.7 p.p.m. could be discerned, the latter being a minor peak. Close inspection of the spectrum revealed weak shoulders near −96, −92 and −83.4 p.p.m., which were assigned as Q^4(2Al), Q^4(3Al) and Q^4(4Al), respectively. Hence, it appears

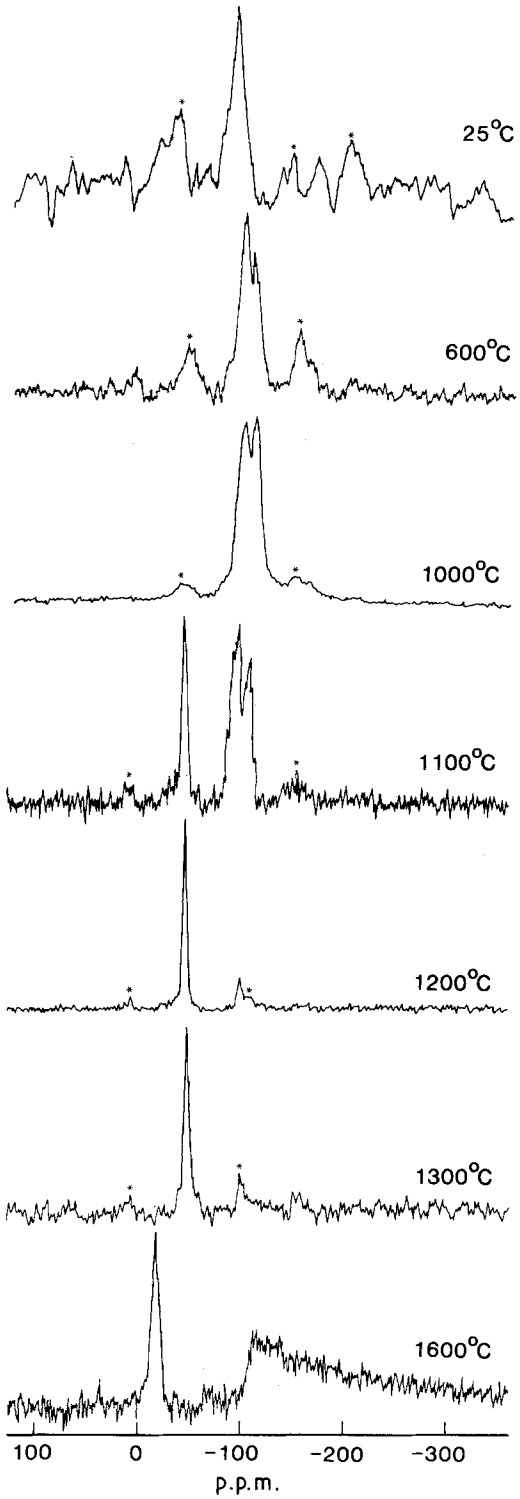

Figure 5 ^{29}Si NMR spectra of C_{12}-Mont/PAN after heating to various temperatures; (*) spinning sidebands.

that silicon had begun to diffuse into the aluminium-rich areas of the original clay structure. After heating the intercalate to 1000 °C, strong absorptions due to Q^4(1Al) at −100.6 p.p.m. and Q^4(0Al) at −110.9 p.p.m. were evident, together with a shoulder at −96.8 p.p.m. (Q^4(2Al)). Resonances due to Q^4(3Al) and Q^4(4Al) could no longer be discerned, suggesting an increasingly even distribution of silicon atoms between Q^4(0Al) and Q^4(1Al) sites. At this stage, all observable silicon was bridged (via oxygen atoms) to four other tetrahedral centres, i.e. in the Q^4 state.

The spectrum after heat treatment of the sample at 1100 °C displayed a sharp resonance at −47.2 p.p.m.

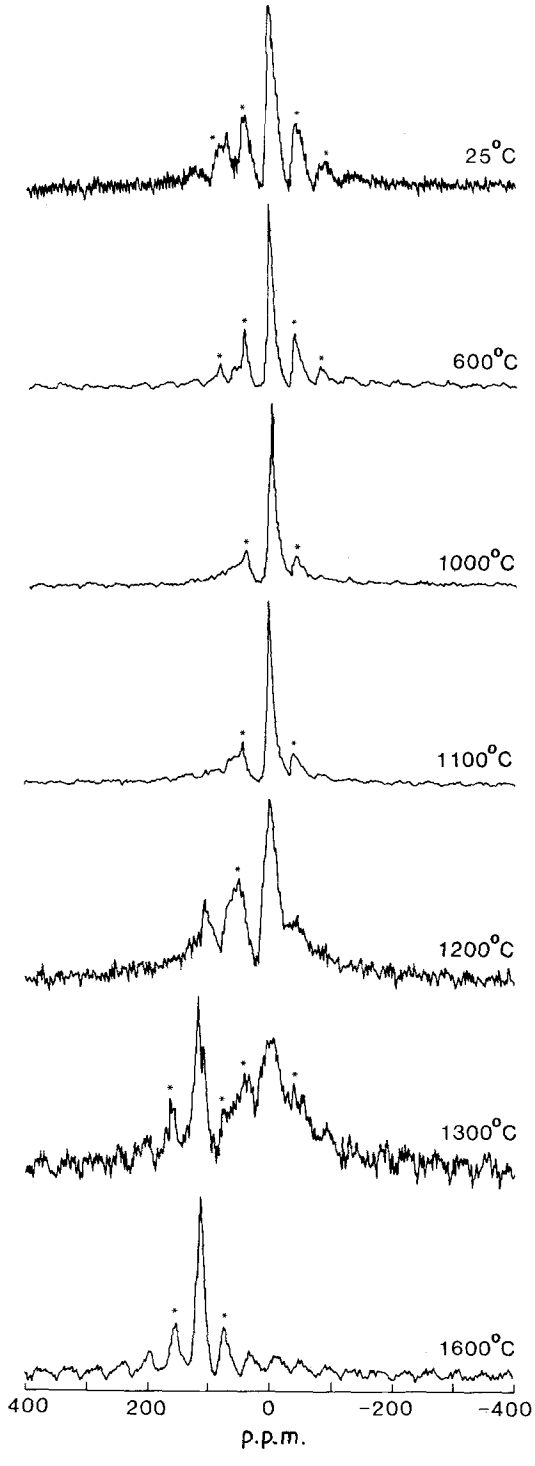

Figure 6 ^{27}Al NMR spectra of C_{12}-Mont/PAN after heating to various temperatures; (*) spinning sidebands.

due to SiN_4 tetrahedra [33], together with a decrease in the intensity of the Q^4(0Al) resonance. The Q^4(1Al) resonance remained strong. After sample reduction at 1200 °C, the SiN_4 resonance in the spectrum had strengthened, and the Q^4(0Al) resonance had disappeared, with only a weak Q^4(1Al) absorption remaining. Reduction of Si–O phases to SiN_4 tetrahedra was complete by 1300 °C.

After sample reduction at 1600 °C, the spectrum displayed two resonances. A single, sharp peak at −18.8 p.p.m. represented the SiC_4 environment of SiC (cubic, 3C polytype) [50], while a very broad resonance near −112.8 p.p.m. was assigned to amorphous SiO_2 [51], probably formed during the subsequent decarbonization step.

The ^{27}Al NMR spectra of C_{12}-Mont/PAN samples (Fig. 6) after heating at temperatures up to 1100 °C were almost invariant; they showed a strong AlO_6 resonance (2.9 p.p.m.) and a weak AlO_4 shoulder (60 p.p.m.). No reduction of the Al–O framework had occurred up to this temperature. After sample reaction at 1200 °C, however, resonances at 50.7 p.p.m. (AlO_4) and 110 p.p.m. (AlN_4) appeared. AlN itself has a resonance at 112.1 p.p.m. [32, 52]. After heating to 1300 °C, the spectrum displayed broad, complex absorptions in the AlN_4, AlO_4 and AlO_6 regions. The resonances in the first two of these regions implied the presence of various Al (O, N)$_4$ tetrahedra (as expected in β′-sialon [32, 52]), while the persistence of an AlO_6 resonance could be due to incomplete reduction of the octahedral Al–O layer and/or the presence of impure amorphous alumina derived from magnesium-containing phases such as $MgAl_2O_4$, after loss of magnesium as metal (see TEM section). After heating the sample to 1600 °C, the ^{27}Al NMR spectrum was identical to that of AlN, indicating complete conversion of the Al–O framework to an AlN_4 environment.

4. Conclusions

NMR and XRD observations in this work generally support previous studies, in showing an increase in reactivity and selectivity for β′-sialon formation, when using a nanocomposite approach [17].

Both Na-Mont and C_{12}-Mont underwent thermal disproportionation into α-cristobalite, cordierite, quartz and mullite above 1000 °C. Similar phenomena occur when physical mixtures of clay and carbon are heated in the presence of nitrogen gas. The carbothermal reduction of the free silica thus formed to SiC, and its subsequent incomplete reaction with mullite, are known to result in an impure β′-sialon containing unreacted mullite, alumina and in some cases, sialon phases other than the β′ series [17, 53]. Alumina, in particular, is relatively difficult to remove by reduction at moderate temperatures.

In contrast, the carbothermal reactions of C_{12}-Mont/PAN appeared to involve decomposition of organics, followed by dehydroxylation of the clay, interlayer carbon formation and structure collapse, in that order, so that by 1000 °C, alternating bands of carbon and amorphous aluminosilicate were produ-

ced [41]. Based on the original montmorillonite structure, and ^{29}Si NMR results, each aluminosilicate slab was relatively silicon-rich near the carbon interface, and aluminium-rich near the centre. These slabs contained aluminium in both tetrahedral and octahedral coordination. Separation of magnesium-containing phases (such as $MgAl_2O_4$) and iron metal occurred by 1000 °C. Above 1000 °C, some of this iron metal may have reacted further to give traces of iron carbides or ferrosilicon. Progressive volatilization of magnesium as the metal occurred above 1100 °C, leaving a residue of amorphous, finely divided material which was probably impure Al_2O_3.

It was expected that reduction of the composite structure would begin near the interface of the carbon and outer regions of the slabs (Si–O-rich regions, mainly $Si(OSi)_4$ environment). This was observed to commence by 1100 °C, to produce SiN_4 tetrahedra in a single step. There was no NMR evidence for the presence of $Si(O,N)_4$ tetrahedra at any stage of the reduction. This may be a kinetic effect, reflecting the rapid nitridation of $Si(O,N)_4$ intermediates to SiN_4 tetrahedra, and/or their disproportionation to SiN_4 and SiO_4 species.

With increasing temperature, subsequent reduction of $Si(OSi)_3(OAl)$ tetrahedra further towards the centre of the slab (formed by progressive diffusion of silicon inwards) occurred. Reduction of the aluminium-rich centre of the slab began above 1100 °C, most likely via diffusion of CO, N_2 and possibly the volatile intermediate SiO into the framework.

By 1200 °C, conversion of the silicon to an SiN_4 environment was essentially complete. Progressive conversion of AlO_6 and AlO_4 sites into the $Al(O,N)_4$ tetrahedra of β′-sialon occurred with increasing temperature. This was accomplished via reduction and nitridation of the Al–O bonds followed by diffusion into the β-Si_3N_4 structure. However, this process was not complete even at 1300 °C, resulting in the persistence of further X-ray-amorphous aluminium-rich material (apart from that derived from $MgAl_2O_4$). Such phases may have included finely divided aluminium nitride and/or oxynitrides (in addition to impure alumina). There was no evidence (at least by diffraction methods) for the formation of any sialon phases other than β′.

By 1300 °C or higher, all flake-like clay-derived material had disappeared, in keeping with the NMR observation that all silicate groups had been nitrided to an SiN_4 environment. In contrast to the carbothermal reduction of kaolinite [53], no evidence was found for the presence of SiC at temperatures up to 1300 °C.

By 1600 °C, all silicon was present as SiC, and all aluminium (including that derived from amorphous impurities) as AlN. The formation of SiC at higher temperatures was consistent with its increased stability relative to β-Si_3N_4 at temperatures above 1400 °C [37].

It is suggested that the presence of interlayer carbon suppressed condensation between neighbouring aluminosilicate slabs (which would otherwise result in the formation of mullite and silica). This factor, together with the high atomic dispersion of the carbon, was probably responsible for lowering the threshold temperature for reduction.

The progressive increase in Si:Al ratio in the products with increasing reaction temperature was attributed to loss of aluminium during the acid extraction procedure. Since there was no spectroscopic evidence (XRD, NMR) for acid degradation of β′-sialon (no change in XRD, absence of silica), it is concluded that loss of aluminium occurred via dissolution of very poorly crystalline alumina, aluminium nitride and possibly aluminium oxynitrides. The first of these was a residue from incomplete reaction, whilst the latter two could have been co-produced (along with β-Si_3N_4 and later SiC) during the reduction process at 1200 °C or higher. All three materials are susceptible to acid attack, especially when finely divided. Of these, only AlN was detected by diffraction, and then only in the sample heated to 1600 °C (both before and after decarbonization/acid treatment). However (if present), this may have reflected its very small particle size at lower temperatures. The presence of alumina (in amorphous form) was implied by AlO_6 resonances observed in the ^{27}Al NMR of samples heated as high as 1300 °C (acid extraction notwithstanding). The presence of aluminium oxynitrides at these temperatures is plausible, although no direct evidence was found. However, by 1600 °C, the complete absence of diffracting alumina and oxynitrides (even before decarbonization and acid extraction) implied that all aluminium was present as AlN by this temperature, since α-Al_2O_3 and aluminium oxynitrides (if present) would be expected to give well-defined XRD patterns by this temperature.

An optimum temperature for β′-sialon production from montmorillonite therefore lies between 1300 and 1600 °C, at which point the extent of reduction of AlO_n environments to $Al(O,N)_4$ tetrahedra would have been maximized before reduction of SiN_4 to SiC_4 environments commenced. A longer reaction time in this temperature range might also increase β′-sialon yields by allowing a greater extent of diffusion of α-Al_2O_3, AlN or aluminium oxynitrides into the β-Si_3N_4 structure.

Acknowledgements

We gratefully acknowledge Dr David Hay for powder XRD patterns, Mr David Watson for electron micrographs and diffraction patterns, Mr Geoff West for obtaining some of the early NMR spectra, Mr Tony McKinnon for elemental analyses, Mr John Newman for thermal analyses and Dr Bruce Poppleton for helpful discussions.

References

1. K. H. JACK, in "Non-Oxide Technical and Engineering Ceramics", edited by Stuart Hampshire (Elsevier, 1986) p. 1.
2. I. J. McCOLM, in "Ceramic Science for Materials Technologists" (Leonard Hill, New York, 1983).
3. K. H. JACK, in "High Technology Ceramics", Vol. 3 of "Ceramics & Civilization", edited by W. D. Kingery (American Chemical Society, 1986).
4. *Idem, J. Mater. Sci.* **11** (1976) 1135.

5. A. J. MOULSON, *ibid.* **14** (1979) 1017.
6. J. B. BALDO, V. C. PANDOLFELLI and J. R. CASARINI, in "Ceramic Powders", edited by P. Vincenzini (Elsevier, Amsterdam, 1983) pp. 437–444.
7. I. L. BOYARINA, A. B. PUCHKOV, A. M. GAURISH, Z. D. ZHUKOVA and E. V. DEGTYAREVA, *Refractories (Engl. Transl.)* **23** (1982) 191.
8. C. J. SPACIE, in "Non-oxide Technical and Engineering Ceramics", edited by Stuart Hampshire (Elsevier Applied Science, 1983) pp. 133–147.
9. J. MUKERJI and S. BANDYOPADHYAY, *Adv. Ceram. Mater.* **3** (1988) 369.
10. J.-G. LEE and I. B. CUTLER, *Amer. Ceram. Soc. Bull.* **58** (1979) 869.
11. S. BANDYOPADHYAY and J. MUKERJI, *Adv. Ceram. Mater.* **3** (1988) 328.
12. S. A. SIDDIQI, I. HIGGINS and A. HENDRY, in "Non-oxide Technical and Engineering Ceramics", edited by Stuart Hampshire (Elsevier Applied Science, 1983) pp. 119–132.
13. F. K. VAN DIJEN, R. METSALAAR and C. A. M. SISKENS, *J. Amer. Ceram. Soc.* **68** (1985) 16.
14. I. HIGGINS and A. HENDRY, *Proc. Br. Ceram. Soc.* **38** (1986) 163.
15. M. E. BOWDEN, K. J. D. MACKENZIE and J. H. JOHNSTON, in "Ceramic Developments", edited by C. C. Sorrell and B. Ben-Nissan (Trans Tech Publications, 1988).
16. Y. SUGAHARA, K. KURODA and C. KATO, *Ceram. Int.* **14** (1988) 1.
17. *Idem, J. Mater. Sci.* **23** (1988) 3572.
18. Y. SUGAHARA, K. SUGIMOTO, K. KURODA and C. KATO, *Yogyo Kyokaishi* **94** (1986) 48.
19. R. H. MEINHOLD, K. J. D. MACKENZIE and I. W. M. BROWN, *J. Mater. Sci. Lett.* **4** (1985) 163.
20. E. LIPPMAA, A. SAMOSON and M. MAGI, *J. Amer. Chem. Soc.* **108** (1986) 1730.
21. D. TILAK, B. TENAKOON, J. M. THOMAS, W. JONES, T. A. CARPENTER and S. RAMDAS, *J. Chem. Soc. Faraday Trans. 1* **82** (1986) 545.
22. J. G. THOMPSON, *Clay Miner.* **19** (1984) 229.
23. D. TILAK, B. TENAKOON, W. JONES and J. M. THOMAS, *J. Chem. Soc. Faraday Trans. 1* **82** (1986) 3081.
24. E. LIPPMAA, M. MAGI, A. SAMOSON, G. ENGELHARDT and A. R. GRIMMER, *J. Amer. Chem. Soc.* **102** (1980) 4889.
25. M. MAGI, E. LIPPMAA, A. SAMOSON, G. ENGELHARDT and A. R. GRIMMER, *J. Phys. Chem.* **88** (1984) 1518.
26. J. B. MURDOCH, J. F. STEBBINS and I. S. E. CARMICHAEL, *Amer. Mineral.* **70** (1985) 332.
27. C. A. WEISS Jr, S. P. ALTANER and R. J. KIRKPATRICK, *ibid.* **72** (1987) 935.
28. J. SANZ and J. M. SERRATOSA, *J. Amer. Chem. Soc.* **106** (1984) 4790.
29. I. W. M. BROWN, K. J. D. MACKENZIE and R. H. MEINHOLD, *J. Mater. Sci.* **22** (1987) 3265.
30. J. SANZ, A. MADANI, J. M. SERRATOSA, J. S. MOYA and S. AZA, *J. Amer. Ceram. Soc.* **71** (1988) C418.
31. C. A. FYFE, J. M. THOMAS, J. KLINOWSKI and G. C. GOBBI, *Angew. Chem. Int. Ed. Engl.* **22** (1983) 259.
32. J. KLINOWSKI, J. M. THOMAS, D. P. THOMPSON, P. KORGUL, K. H. JACK, C. A. FYFE and G. C. GOBBI, *Polyhedron* **3** (1984) 1267.
33. R. S. AUJLA, G. LENG-WARD, M. H. LEWIS, E. F. W. SEYMOUR, G. A. STYLES and G. W. WEST, *Phil. Mag. B* **54** (1986) L51.
34. T. TAKI, M. INUI, K. OKAMURA and M. SATO, *J. Mater. Sci. Lett.* **8** (1989) 918.
35. M. I. ATTALA, L. A. BRUCE, S. I. HODGSON, T. W. TURNEY, M. A. WILSON and B. D. BATTS, *Fuel* **69** (1990) 725.
36. C. DOBLIN, personal communication (1989).
37. S. A. SIDDIQI and A. HENDRY, *J. Mater. Sci.* **20** (1985) 3230.
38. J. W. EARLEY, I. H. MILNE and W. J. McVEAGH, *Amer. Mineral.* **38** (1953) 770.
39. "Chemistry of Clays and Clay Minerals", edited by A. C. D. Newman, Mineralogical Society Monograph No. 6 (Longman, 1987) pp. 321, 355.
40. *Ibid.*, p. 312.
41. Y. SUGAHARA, K. KURODA and C. KATO, *J. Amer. Ceram. Soc.* **67** (1984) C247.
42. J. W. EARLEY, B. B. OSTHAUS and I. H. MILNE, *Amer. Mineral.* **38** (1953) 707.
43. W. F. BRADLEY and R. E. GRIM, *ibid.* **36** (1951) 182.
44. R. E. GRIM and G. KULBICKI, *ibid.* **46** (1961) 1329.
45. G. KULBICKI, *Clays Clay Miner.* **5** (1958) 144.
46. G. ENGELHARDT, D. ZEIGAN, H. JANCKE, D. HOEBBEL and W. WIEKER, *Z. Anorg. Allg. Chem.* **418** (1975) 17.
47. G. ENGELHARDT, H. JANCKE, D. HOEBBEL and W. WIEKER, *Z. Chem.* **14** (1974) 109.
48. I. W. M. BROWN, K. J. D. MACKENZIE, M. E. BOWDEN and R. H. MEINHOLD, *J. Amer. Ceram. Soc.* **68** (1985) 298.
49. J. V. SMITH and C. S. BLACKWELL, *Nature* **303** (1983) 223.
50. G. R. FINLAY, J. S. HARTMAN, M. F. RICHARDSON and B. L. WILLIAMS, *J. Chem. Soc. Commun.* (1985) 159.
51. M. A. WILSON, in "NMR Techniques and Applications in Geochemistry and Soil Chemistry" (Pergamon, 1987) p. 117.
52. N. D. BUTLER, R. DUPREE and M. H. LEWIS, *J. Mater. Sci. Lett.* **3** (1984) 469.
53. I. HIGGINS and A. HENDRY, *Trans. J. Br. Ceram. Soc.* **85** (1986) 161.

Received 5 February
and accepted 19 February 1990